ANTINEUTRINO DETECTOR CONCEPTS FOR SAFEGUARDING SPENT NUCLEAR FUEL REPOSITORIES

AUTHORS

Y. SCHNELLBACH
RWTH Aachen University
Aachen, Germany
schnellbach@nvd.rwth-aachen.de

T. RADERMACHER
RWTH Aachen University
Aachen, Germany

I. NIEMEYER
Forschungszentrum Jülich
Jülich, Germany

S. ROTH
RWTH Aachen University
Aachen, Germany

M. GÖTTSCHE
RWTH Aachen University
Aachen, Germany

ABSTRACT

Spent nuclear fuel (SNF) from nuclear power generation requires long-term safeguarding in dedicated storage facilities and geological repositories. Current safeguards approaches use a combination of containment and surveillance, and design information verification. Antineutrino emissions from the ongoing beta decay of fission fragments provide a potential complementary information on potential diversion of nuclear material or misuse of the facility, as antineutrinos pass through any shielding, structure, or geology effectively unhindered.

This study investigates a novel antineutrino detection concept using a liquid-organic (LOr) time projection chamber (TPC), combining scalability and high-resolution particle reconstruction of TPCs with the large quantity of target hydrogen atoms provided by organic compounds. Geant4- based simulations and subsequent modelling of the electron drift behavior are used to understand inverse beta decay (IBD) event topologies and reconstruction in an ISO container-sized concept detector. The concept detector's expected signal rate, sensitivity to inventory changes and directional capabilities are then estimated for a representative example repository with varying deployment distances and scenarios. This estimation is compared to other state-of-the-art antineutrino detection technologies, including liquid and segmented plastic scintillation detectors, that have been proposed for nuclear monitoring. This comparison will be used to determine the feasibility and suitability of antineutrino detectors currently under development as complementary safeguards measure for final disposal of SNF in geological repositories.

1. INTRODUCTION

During the operation of nuclear reactors, spent nuclear fuel (SNF) is produced. The SNF is periodically discharged from a reactor core as part of the refueling process. This SNF is then transferred and stored in spent fuel ponds for several years until its radioactivity and decay heat reduces and is then either transferred into interim storage or to reprocessing facilities. It is planned to, ultimately, dispose of SNF in geological repositories. The first facility of this kind is expected to start operation in this decade.

In 2021, it was estimated that the global annual accumulation of SNF was ~7,000 t of heavy metal (t HM), with the total stored inventory being ~300,000 t HM [1]. SNF from commercial sources mainly consists of ~93-96% uranium, mostly ^{238}U but also small (<1%) amounts of ^{235}U, ~4% fission fragments, ~1% plutonium (^{239}Pu, ^{241}Pu), and <1% minor actinides [2]. Special fissionable material must be safeguarded to prevent diversion, especially of significant quantities, defined as 8 kg of Pu,

8 kg of ^{233}U or 25 kg of highly enriched uranium (HEU, ^{235}U > 20%) [3]. Due to the large quantities of SNF produced, this means significant quantities of special fissionable material are present in SNF storage, including interim storage facilities and geological repositories and therefore require comprehensive safeguards.

Currently, SNF from commercial reactors and research reactors under safeguards obligations is usually verified by the safeguards authorities, through measurements before being transferred to dry interim storage. This nuclear material accountancy is then combined with safeguards measures such as design information verification (DIV) and containment and surveillance (C/S) techniques in spent fuel storage facilities (SFSFs) [4]. Furthermore, accurate material accountancy relies on continuity of knowledge (CoK) and is a key element of safeguards, hence methods of re- verification after a loss of CoK are also being investigated. Two such methods are muography and fast neutron imaging [5, 6]. It is likely that future geological repositories will rely on the geological containment provided by its underground location combined with DIV, geophysical monitoring, and C/S techniques. New or novel techniques under considerations are microseismic monitoring, ground penetrating radar and Kr-85 monitoring [7].

Another avenue of monitoring SNF that has been proposed is antineutrino detection [8, 9], exploiting the continuous emission of antineutrinos by the fission fragments in SNF. Due to their low interaction rate with matter [10], antineutrinos can penetrate shielding and containment, leading to a detectable signal correlated with the contents of the SNF in storage. This information is complementary to the information delivered by the other safeguards methods and has the potential to increase redundancy and assist with reverification in case of loss of CoK. The monitoring of nuclear reactors has been proposed in the past [11, 12, 13] and led to several experiments detecting antineutrino emissions from active reactors [14, 15]. However, due to the lower antineutrino rates and energies from SNF, the use of antineutrino monitoring for safeguarding geological repositories must be studied in detail.

2. DETECTION OF ANTINEUTRINOS FROM SPENT NUCLEAR FUEL

Fission fragments in nuclear fuel undergo beta decays, releasing electron antineutrinos. The Q- value of the decay determines the total energy available to the decay radiation. Additionally, the decay rate is approximately proportional to the fifth power of the Q-value [16], meaning decays with the highest energy available to the emitted antineutrino are often decaying away within a short period of time after the initial fission. As a result, the antineutrino flux from SNF is several orders of magnitude lower than the flux from active reactor core and the energy spectrum shifts towards lower energy antineutrinos.

Furthermore, antineutrinos typically produced in SNF beta decays exhibit a very low interaction cross section of ~10^{-41} cm^{-2}. This means the antineutrino emissions cannot be shielded, deflected, or scattered by the containment or geology of the repository. While this presents a unique advantage of an antineutrino-based approach, this also presents a challenge for detection, due to the resultant low signal rates. Low-energy antineutrinos are typically detected via the Inverse Beta Decay (IBD) channel:

$$\overline{\upsilon_e} + p \longrightarrow e^+ + n$$

The outgoing positron carries an energy proportional to the antineutrino energy, immediately deposits it via ionization of the surrounding material and then annihilates with an electron in the medium, releasing two 511 keV photons back-to-back. The neutron undergoes a random walk through the material, scattering off nuclei and losing its energy via thermalization for several microseconds until

it is captured by a nucleus. The capture nucleus is left in an excited state and deexcites via the release of photons, such as a single 2.2 MeV photon when captured by hydrogen.

This distinct double coincident signal of a prompt positron track and annihilation and a delayed neutron capture allows for effective background rejection, while theoretically allowing reconstruction of the original antineutrino given a sufficiently detailed reconstruction of the final state particles: the energy can be determined through measuring the energy of the positron, while the original direction of the neutron before scattering is strongly correlated with the antineutrino direction. However, while IBD is an effective detection channel used in many detectors, it also has a minimum energy threshold of 1.8 MeV. Especially for SNF, this threshold is above the antineutrino energy of most long-lived fission fragments.

The main backgrounds expected in IBD detection are two-fold: other antineutrino sources and fast neutrons. Geoneutrinos as well as operating reactors also emit antineutrinos in the energy window of interest. These backgrounds result in identical event signatures but good knowledge of the expected background rates can be used to estimate the background rate. Furthermore, direction reconstruction of the incoming antineutrino can also be used to minimize the impact of these backgrounds, hence, directionality is a desired ability of a safeguards-motivated antineutrino detector. Fast neutron background is usually due to the neutron activation by cosmic rays, releasing a neutron that can, together with an accidental, mimic the double-coincident time structure of an IBD event. This background can be reduced through a combination of high radiopurity detector materials, detector shielding and/or overburden and improved spatial reconstruction of the prompt positron to distinguish it from electrons produced in beta decays.

3. ANTINEUTRINO SPECTRA FROM SPENT NUCLEAR FUEL

To qualify and quantify the expected signal from SNF repositories, the emission spectrum from SNF as well as its evolution over time is simulated. Several decay chains are present for decades to centuries and of main interest to SNF, such as ^{90}Sr and ^{137}Cs with half-lives of 28.8 and 30.1 years, respectively. Of particular interest is ^{90}Sr, as it decays to ^{90}Y, which has a high decay energy of 2.28 MeV. As ^{90}Sr and ^{90}Y are in secular equilibrium, the half-life of ^{90}Sr effectively dictates the abundance of ^{90}Y and hence the antineutrino flux.

The isotopic composition of a fuel element at the time of discharge is simulated using the OpenMC-based ONIX simulation code [17, 18], followed by its decay. For the purposes of this study, a GKN II fuel assembly [19] with a burn-up of 54 MWd/kg is assumed. After the extraction from the reactor, the isotopic composition of the fuel elements is simulated further at varying time steps up to 300 years from discharge. During this period, the simulation assumes no further burn-up and only continuing decay of the isotopes present. The isotopic composition is transformed into antineutrino emissions by evaluating the dominant contributions to the antineutrino flux [8], shown in Table 1. The activity of each isotope is calculated to determine flux, while the spectral shape is evaluated via reference beta spectra in the NDS ENSDF database [20, 21], originally calculated using BetaShape [22, 23]. The resultant spectra are then convolved with the IBD cross-section to determine the antineutrino interaction rate per target proton with respect to energy and age of the SNF. This allows the scaling of the expected antineutrino interaction rate in a target detector, based on the detector parameters.

Isotope	$t_{1/2}$ [years]	Activity [TBq/kg]	Maximum $E_{\bar{\nu}}$[1] [MeV]	Abundance at t=0 [kg/ton]	Abundance at t=10y [kg/ton]
^{137}Cs	30.1	3.2×10^{3}	1.18	1.68	1.33
^{106}Ru	1.02	1.23×10^{5}	3.54	1.59×10^{-1}	1.78×10^{-4}
^{90}Sr	28.8	5.11×10^{3}	2.28	6.92×10^{-1}	5.44×10^{-1}

Table 1: *Dominant antineutrino-emitting isotopes in spent nuclear fuel 10+ years after discharge from reactor.*

4. COMPARED DETECTOR TECHNOLOGIES

For this study, several detector technologies are being considered, using previous experiments as guidance. Detectors proposed or used for the detection of reactor neutrinos in the past have utilized scintillators [14, 15], in liquid or plastic form, water Cherenkov tanks [24], radiochemical techniques [25] and time projection chambers (TPCs). While successful in the past, Cherenkov tanks and radiochemical techniques have been excluded from the use for SNF monitoring. Water Cherenkov methods are excluded due to the strict geometric constraints on tanks and due to the Cherenkov radiation threshold in water for electrons and positrons at ~0.8 MeV. As the positron energy is related to the antineutrino energy by $E_e = E_\nu - \Delta_m$, where Δ_m= 1.29 MeV is the mass difference between protons and neutrons, this results in an effective detection threshold of ~2.09 MeV, removing most of the ^{90}Sr/^{90}Y signal as well as excluding detection of the annihilation photons. Radiochemical techniques rely on the accumulation of the IBD process products and hence neither allow an event-by-event detection nor a continuous monitoring signal – both highly desirable for a monitoring system detecting anomalies.

Hence, two technologies considered here are based on organic scintillators, either in the form of a liquid or plastic. Both approaches have been deployed experiments at civil or research reactor sites, demonstrating that the technology can be used at nuclear sites, and use large amounts of hydrogen-rich detection material, acting as semi-free protons for the IBD process. Based on a survey of the existing reactor experiments, the scintillation media chosen for comparison are linear alkylbenzene (LAB), a liquid scintillator used by several neutrino experiments, and polyvinyl toluene (PVT), a common base material for plastic scintillators [26]. Another technology considered are liquid-organic time projection chambers (LOr-TPCs), combining the advantages of time projection chambers, the ability to fully reconstruct each particle in the final state with high spatial resolution, with the advantages of an organic liquid, providing a dense hydrogen-rich target material at room temperature. Key properties of all candidate detector media are shown in Table 2.

Detector Medium	Chemical Formula	Density [g/cm^3]	H-atoms/m^3
LAB	$C_6H_5C_nH_{2n+1}$	0.86	7.5×10^{28}
PVT	$[CH_2CH(C_6H4CH_3)]_n$	1.10	4.5×10^{28}
TMS	$Si(CH_3)_4$	0.65	5.3×10^{28}

Table 2: *Key properties of selected detector media investigated for use in IBD channel antineutrino detectors.*

5. IBD EVENTS IN LIQUID ORGANIC TIME PROJECTION CHAMBERS

The LOr-TPC concept uses the underlying principle of TPCs but uses an organic dielectric liquid as interaction and drift medium. The candidate liquid under investigation is tetramethylsilane (TMS), $Si(CH_3)_4$, a non-polar organic liquid with spherical molecules. Unlike liquefied noble gasses used in

[1] Maximum $E_{\bar{\nu}}$ emitted in the decay subsequent decay chain, except for ^{137}Cs, where the antineutrino is emitted by the decay of ^{137}Cs directly.

other TPC-based neutrino experiments [27, 28], it is liquid at room temperature, avoiding the need for a cryostat. TMS has been studied for use in calorimeter detectors [29, 30] and has been proposed as material for TPCs [31], including initial experiments to determine its relevant properties [32]. However, there are still open questions, especially concerning its scalability and drift behavior in large-scale experiments.

Drift Parameter	**Value**
Maximum drift length	1 m
Sensitive volume	80 m^3
Electric drift field	5.0 kV/cm
Drift velocity	5.5 µm/ns
Diffusion coefficient	60 µm/cm^{-2}
Electron yield	7 electrons/keV
Pad size	5 mm × 5mm

***Table 3**: Simulation parameters for electron drift simulation in TMS.*

To determine whether IBD events can be observed with sufficient fidelity to be reconstructed, the antineutrino spectra have been used to simulate interactions with a TMS target using the GENIE neutrino event generator [33]. The outgoing positron and neutron of the IBD process have then been simulated in a TMS volume using GEANT4 [34, 35] to determine the energy deposition within the medium. This information is then used to calculate the number of created ionization electrons and the expected signal at the anode, assuming the drift properties shown in Table 3. Simulations have shown that the energy depositions from the different final state particles are well-separated, as shown in the example event in Figure 1.

The positron track starts at the primary interaction vertex, typically producing a track of less than 1 mm. Despite the short length and low energy (<500 keV kinetic energy), the signal is up to 3200 electrons, allowing a clear identification of the positron and primary vertex. The annihilation photons themselves produce no signal, but Compton electrons can be detected as they lose energy in the medium. The neutron scatters off nuclei in the medium, inducing proton recoils that result in ~8.4 electrons on the first recoil. Since the vector between the primary vertex and this recoil indicates the original neutron direction after the IBD process, this direction also indicates the original antineutrino direction.

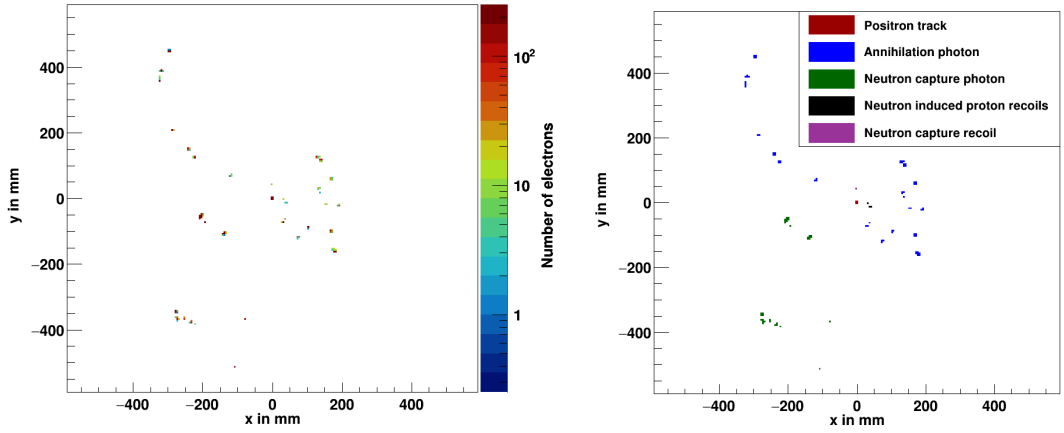

***Figure 1:** Example IBD event in TMS projected on an anode at 1 m distance to the primary IBD vertex, showing the electron yield (left) and the associated particles (right). [36]*

Due to the high hydrogen content, 93% of the neutrons are capturing on hydrogen, releasing a 2.2 MeV photon, which also leaves a clear, time-delayed signal in the medium. Studies have shown that, if this signal can be fully resolved, it is possible to reconstruct the original antineutrino direction with less than 10° deviation in 88% of all events [36].

6. INITIAL SENSITIVITY STUDIES FOR NUCLEAR STORAGE SITES

To compare expected antineutrino rates and sensitivities, two simplified sites have been studied, one based on an interim storage facility, and one based on a geological repository. For both studies, the same GKN II fuel assemblies described above are used. The simulated detectors are assumed to have a fiducial volume of 80 m^3, roughly the volume offered by an instrumented 40 ft. shipping container and use TMS as detection medium unless noted otherwise.

The simplified interim storage site is based on an existing interim storage facility [37]. This interim storage site can hold up to 130 fuel casks at full occupancy, with each cask holding 19 fuel assemblies for a total storage of up to 2,470 fuel assemblies if fully occupied. The casks are distributed in 5 rows and 26 columns, with each storage position separated by 3.5 m. It is assumed that SNF has been stored over time, with a fifth of the SNF having been stored 20, 30, 40, 50, and 60 years ago respectively. Four detectors are placed outside the repository at 10 m distance to the casks as shown in Figure 2.

The simplified geological repository site uses a layout motivated by past exploratory studies for a geological repository site in Germany [38]. The simplified geological repository site is based on a section of the plans of the exploratory mine and holds 1,120 casks, each containing 10 fuel assemblies for a total of 11,200 fuel assemblies. The casks are distributed in 10 rows and 112 columns, with each row separated by 36 m and each column by 8.15 m. Here, eight detectors are simulated 50 m above the repository and are assumed to be evenly distributed across the repository, shown in Figure 3.

For comparison purposes, detector efficiency effects and non-neutrino backgrounds are neglected since these effects are dependent on the exact detector configuration and readout technology. Antineutrino backgrounds from geoneutrinos and reactor antineutrinos have been estimated to be in the range of 0.86 to 1.43 events per detector per year based on current models [39] and are therefore also neglected.

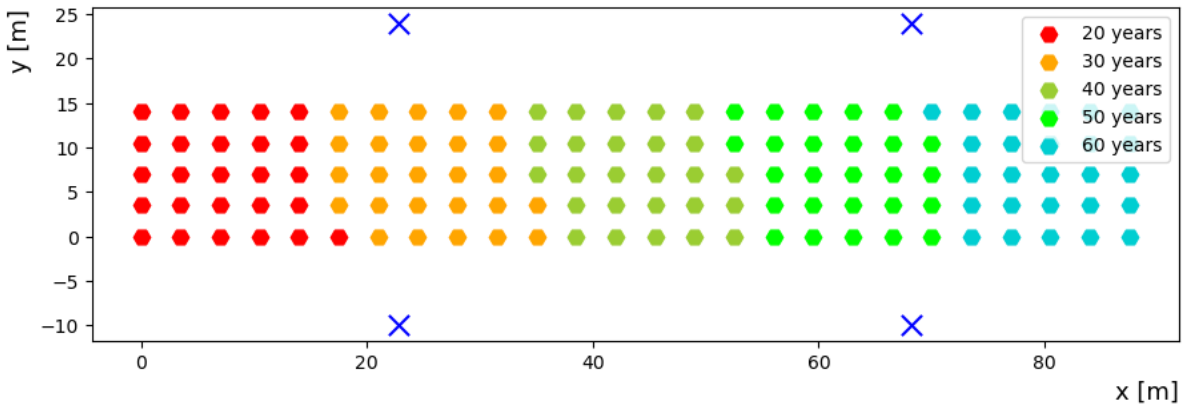

***Figure 2**: Simplified interim storage site housing 130 casks, distributed across 5 rows and 26 columns. Each cask contains 19 fuel assemblies, totaling 2,470 fuel assemblies. The SNF has been divided into five equal-sized groups, stored for 20, 30, 40, 50 and, 60 years. The blue crosses mark the position of the detectors.*

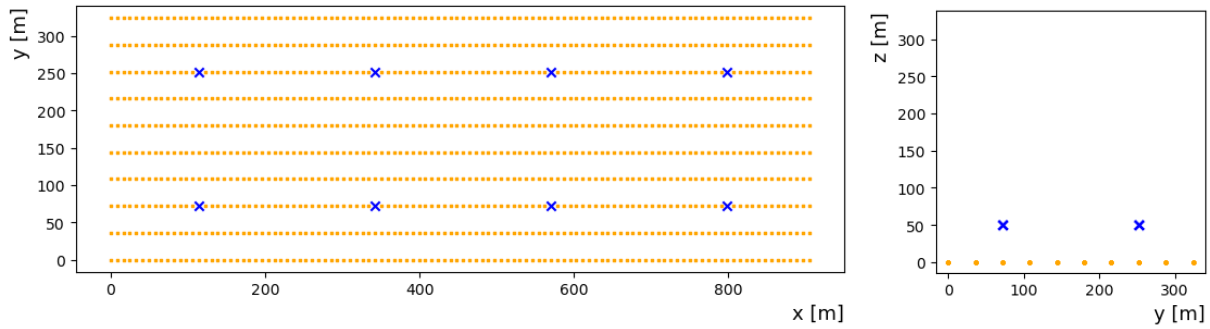

Figure 3: *Arrangement of 10 rows and 112 columns of fuel cask in the simplified geological repository, shown in the x-y plane (left) and y-z plane (right). Each cask contains 10 fuel assemblies, totaling 11,200 fuel assemblies across the entire modelled repository. The blue crosses indicate the position of the detectors, 50 m above the repository.*

The interaction rates for the three investigated detection media have been compared for both simplified sites by determining the monthly rate of interactions in a single detector for a range of SNF ages, assuming all casks have been discharged at the same time. Due to the lack of symmetry between the detector positions in the site, the interaction rates vary between detector locations. The three compared detection media display similar interaction rates as shown in Figure 4 and exhibit the expected exponential drop-off with time. Especially for the geological repository site, it is notable that after ~250 years, the expected interaction rate at ~50 m distance falls below a single monthly event for the studied detector configuration.

To understand the sensitivity to changes in the inventory, the removal of material serves as benchmark. For the interim storage site, the diversion of one cask (~10.6 t HM) and the diversion of half the fuel assemblies in a cask have been simulated. In the first scenario, the diversion can be detected with a 90+ % confidence level (CL) after 6.4 months on average, varying between 0.8 and 18.3 months depending on the age and location of the cask, as shown in Figure 5. In the second case, detection takes, on average, 10.7 months with a range of 0.8 to 55.7 months, also shown in Figure 5.

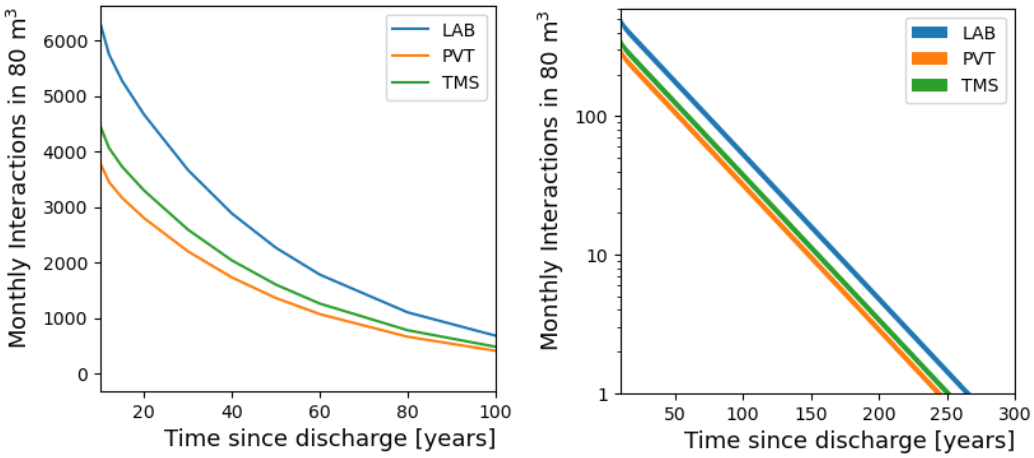

Figure 4: *Monthly antineutrino interaction rates in a single 80m³ detector for the interim storage site (left) and the geological repository site (right), equal age of all fuel assemblies. The colored bands indicate the range of interaction rates for different detector locations.*

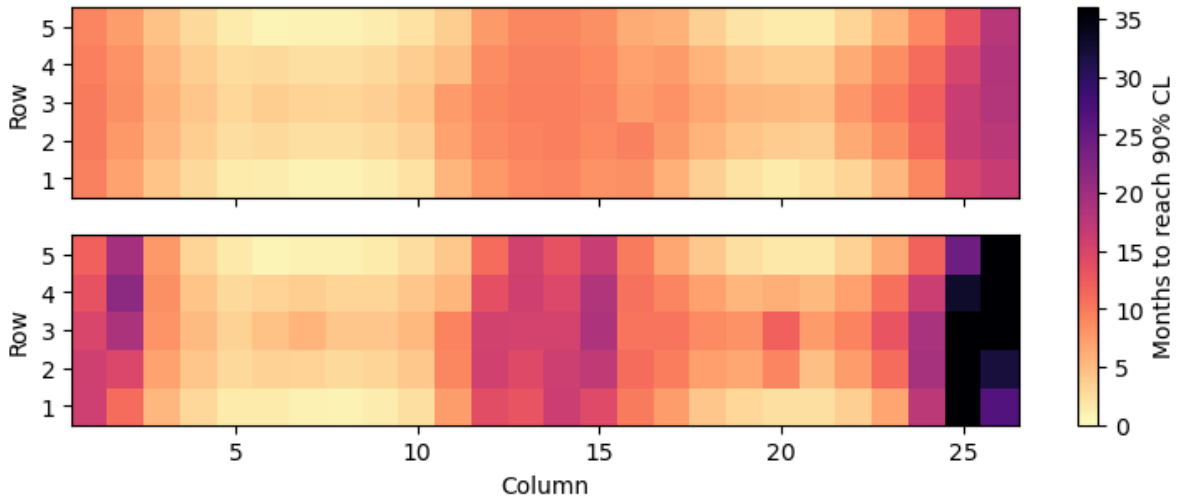

Figure 5: *Time required to detect the removal of a single cask (top) or the contents of half a cask (bottom) at the indicated location with 90+% CL at the interim storage facility.*

For the simplified geological repository site, the casks have been divided into 80 groups, each holding 1.25% of the total repository content (~78.4 t HM). The SNF in the repository is assumed to be disposed at the same time, 50, 100 or 200 years ago. For SNF disposed 50 years ago, the removal of one group of casks can be detected with 90+ % CL after 8.7 months on average, varying between 4.9 and 13.3 months depending on location. For SNF disposed 100 years ago, the diversion can be detected after 14.3 months on average, with a range of 10.3 to 18.1 months, and for SNF disposed 200 years ago, it takes on average 20.6 months to detect the diversion, with a range from 19.3 to 22.0 months, as shown in Figure 6.

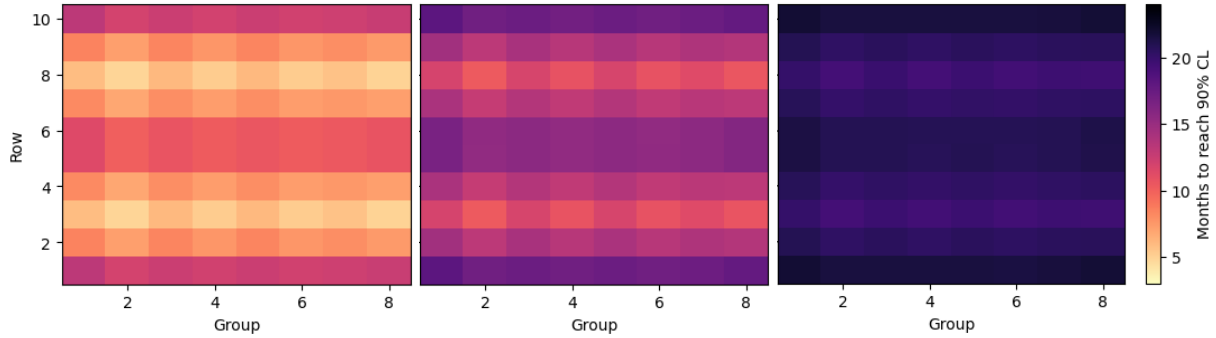

Figure 6: *Time required to detect the removal of a group of casks (1.25% of repository contents) at the indicated location with 90+% CL. All casks are assumed to have been stored for 50 years (left), 100 years (centre) or 200 years (right).*

CONCLUSIONS & OUTLOOK

As geological repositories for spent nuclear fuel become a reality, with the first operational one expected in Finland in this decade, there is renewed interest and demand for new and novel technologies to enhance nuclear safeguards for these new kinds of facilities with an ever-increasing inventory and long filling and storage times. This paper investigates antineutrino-based safeguards approaches and builds upon previous work by identifying potential antineutrino detector technologies for safeguards application and investigating the sensitivity of an idealized detector.

Two simplified SNF storage sites have been modelled and studied, showing that the diversion of a single cask from an interim storage facility can be detected with 90% CL within several months, while changes in a geological repository require longer dwell times. These relatively long dwell times indicate that efficient antineutrino monitoring based on scalar rate measurements alone is very challenging, especially considering the added complexity and required R&D compared to established safeguards technologies. However, the ability to detect nuclear material diversion in an interim storage site in under a month in ideal conditions, hints at the potential antineutrino measurements could have for independently validating the correctness of the declared state of a repository or for investigating suspected deviations, both without requiring physical access to the interior of the facility.

To fully understand the potential benefits antineutrino detectors could provide, future work will explore more sophisticated detector arrangements and the inclusion of additional information, such as directionality, together with a broad survey of safeguards-relevant use cases. Some possible applications could be long-term monitoring of the filling and emptying process, re-verification in the case CoK is lost, or other scenarios where additional independent measurements are desirable. These findings will be used to assess whether antineutrino-based technology can be incorporated into safeguards concepts to further enhance the overall reliability and robustness of these concepts.

ACKNOWLEDGMENTS

We thank Johannes Bosse, Sarah Friedrich, Helge Haveresh, Georg Schwefer, Hannah-Lea Tegtmeyer for previous contributions to the project, which have served as foundation for this work. The research has been funded and supported by the Federal Ministry for the Environment, Nature Conservation, Nuclear Safety and Consumer Protection (BMUV) Grant Number 02W6281 (NU-SAFEGUARDS). Malte Göttsche and Thomas Radermacher have also been funded by a VolkswagenStiftung Freigeist Fellowship.

REFERENCES

[1] IAEA, “Nuclear Technology Review 2021,” in *GC(65)/INF/2*, 2021.

[2] J. Bruno, L. Duro and F. Diaz-Maurin, “Spent Nuclear Fuel and Disposal,” in *Advances in Nuclear Fuel Chemistry*, Woodhead (2022), 527-553.

[3] IAEA, IAEA Safeguards Glossary, IAEA (2022).

[4] IAEA, International Safeguards in the Design of Facilities for Long Term Spent Fuel Management, IAEA (2018).

[5] Vaccaro, S. *et al.*, “Spent fuel cask reverification. Brief technology survey for an integrated multi-method toolkit.,” in *ESARDA 41st Annual Meeting, Symposium on Safeguards and Nuclear Material Management* (2019).

[6] Aymanns, K. *et al.*, “New Technologies for Safeguarding Spent Fuel Storage Facilities,” in *14th Symposium on International Safeguards* (2022).

[7] Khrustralev, K. *et al.*, “Investigations of novel technologies for safeguarding geological repositories,” in *2021 INMM & ESARDA Joint Annual Meeting* (2021).

[8] V. Brdar, P. Huber and J. Kopp, “Antineutrino Monitoring of Spent Nuclear Fuel,” *Phys. Rev. Appl.* **8** (2017).

[9] M. Wittel and M. Göttsche, “Antineutrino Detection Techniques for Monitoring Long-Term Geological Repositories,” in *ESARDA Bulletin 60* (2020).

[10] A. Strumia and F. Vissani, “Precise quasieleastic neutrino/nucleon cross-section,” *Phys. Lett. B* **564** (2003).

[11] A. Borovoi and L. Mikaelyan, “Possibilities of the practical use of neutrinos,” *Sov. At. Energy* **44** (1978).

[12] Korovkin, V.A. *et al.*, “Measuring nuclear power plant output by neutrino detection,” *Sov. At. Energy* **65** (1988).

[13] Akindele, T. *et al.*, “Nu Tools: Exploring Practical Roles for Neutrinos in Nuclear Energy and Security,” PNNL (2021).

[14] Bowden, N. *et al.*, “Experimental results from an antineutrino detector for cooperative monitoring of nuclear reactors,” *Nucl. Instrum. Meth. A* **572** (2007).

[15] Haghighat, A. *et al.*, “Observation of Reactor Antineutrinos with a Rapidly Deployable Surface-Level Detector,” *Phys. Rev. Appl.* **13**, 034028 (2020).

[16] K. Takahashi, M. Yamada and T. Kondoh, “Beta-Decay Half-Lives Calculated on the Gross Theory,” *Atomic Data and Nuclear Data Tables* **12**, 101-142 (1973).

[17] P. Romano, N. Horelik, B. Herman, A. Nelson, B. Forget and K. Smith, “OpenMC: A State-of-the-Art Monte Carlo Code for Research and Development,” *Ann. Nucl. Energy* **82**, 90-97 (2015).

[18] J. de Lanversin, M. Kütt and A. Glaser, “ONIX: An open-source depletion code,” *Ann. Nucl. Energy* **151** (2021).

[19] R. Zahoransky, “Kernkraftwerke,” in *Energietechnik*, Vieweg+Teubner (2004), 86.

[20] IAEA Nuclear Data Services, “Relational ENSDF,” 4 2022. [Online]. Available: https://www-nds.iaea.org/relnsd/NdsEnsdf/QueryForm.html. [Accessed 15 2 2023].

[21] “ENSDF Database,” 4 2022. [Online]. Available: https://www.nndc.bnl.gov/ensdf/.

[22] X. Mougeot, “Reliability of usual assumptions in the calculation of \beta and \nu spectra,” *Phys. Rev. C* **91**, 055504 (2015).

[23] X. Mougeot, “Towards high-precision calculation of electron capture decays,” *Appl. Rad. and Isotopes* **154**, 10884 (2019).

[24] A. de Gouvea and I. Martinez-Soler, “Reactor antineutrino oscillations at Super-Kamiokande,” *Phys. Lett. B* **809**, 135751 (2020).

[25] C. Cowan, F. Reines, F. Harrison, H. Kruse and A. McGuire, “Detection of the Free Neutrino: a Confirmation,” *Science* **124**, 103 (1956).

[26] J. Birks, The Theory and Practice of Scintillation Counting, Pergamon Press (1964).

[27] MicroBooNE Collaboration, “Design and Construction of the MicroBooNE Detector,” *JINST* **12**, P02017 (2017).

[28] DUNE Collaboration, “Deep Underground Neutrino Experiment (DUNE), Far Detector Technical Design Report,” *JINST* **15**, T08008 (2020).

[29] Gonidec, A. *et al*., “Ionization chambers with room temperature liquids for calorimetry,” CERN-EP-88-36, CERN (1988).

[30] Engler, J. *et al*., “A warm-liquid calorimeter for cosmic-ray hadrons,” *Nucl. Instrum. Meth. A* **427**, 528-542 (1999).

[31] J. Dawson and D. Kryn, “Organic Liquid TPCs for Neutrino Physics,” *JINST* **9**, P07002 (2014).

[32] Wu, S. *et al.*, “A Tetramethylsilane TPC with Cherekov light readout and 3D reconstruction,” *Nucl. Instrum. Meth. A* **972**, 163904 (2020).

[33] Andreopoulos, C., “The GENIE Neutrino Monte Carlo Generator,” *Nucl. Instrum. Meth. A* **614**, 87-104 (2010).

[34] Agostinelli, S. *et al.*, “Geant4 - a simulation toolkit,” *Nucl. Instrum. Meth. A* **506**, 250-303 (2003).

[35] Allison, J. *et al.*, “Recent developments in Geant4,” *Nucl. Instrum. Meth. A* **835**, 186-225 (2016).

[36] T. Radermacher, J. Bosse, S. Friedrich, M. Göttsche, S. Roth and G. Schwefer, “Liquid-organic time projection chamber for detecting low energy antineutrinos,” arXiv:2203.01090 [physics.ins-det] (2022).

[37] Kernkraftwerke Lippe-Ems GmbH, “Kurzbeschreibung des Standort-Zwischenlagers Lingen am Kernkraftwerk Emsland,” (1999).

[38] W. Bollingfehr, W. Filbert, C. Lerch and M. Tholen, “Endlagerkonzepte - Bericht zum Arbeitspaket 5,” GRS (2011).

[39] A. Barna and S. Dye, “Antineutrino Model” (2010). [Online]. Available: https://reactors.geoneutrinos.org. [Accessed 13 04 2023].